Title: Environmental tracers to evaluate groundwater residence times and water quality risk in shallow unconfined aquifers in sub Saharan Africa

Authors:

Eddie W. Banks [1], Peter G. Cook [1], Michael Owor [2], Joseph Okullo [2], Seifu Kebede [3], Dessie Nedaw [4], Prince Mleta [5], Helen Fallas [6], Daren Gooddy [7], Donald John MacAllister [6], Theresa Mkandawire [8], Patrick Makuluni [8], Chikondi E. Shaba [9] and Alan M. MacDonald [6]

Affiliations:

[1] National Centre for Groundwater Research and Training and College of Science and Engineering, Flinders University, GPO Box 2100 Adelaide 5001, South Australia, Australia.

[2] Department of Geology and Petroleum Studies, Makerere University, Kampala, Uganda.

[3] University of KwaZulu Natal, Center for Water Resources Research, Pietermartizburg, Private Bag X01, Scottsville, South Africa.

[4] School of Earth Sciences, Addis Ababa University, Addis Ababa, Ethiopia.

[5] Department for Water Resources, Ministry of Agriculture, Irrigation and Water Development, Government of Malawi.

[6] British Geological Survey, the Lyell Centre, Research Avenue South, Edinburgh, EH14 4AS, Scotland, United Kingdom.

[7] British Geological Survey, Maclean Building, Crowmarsh Gifford, Wallingford, Oxfordshire OX10 8BB, United Kingdom.

[8] University of Malawi, The Polytechnic, Private bag 303, Blantyre 3, Malawi.

[9] University of Malawi, Chancellor College, PO Box 280, Zomba, Malawi.

Corresponding author:

Eddie W. Banks, *eddie.banks@flinders.edu.au*

STUDY AREAS

Ethiopia

Ethiopia is in the tropics, located between the Tropic of Cancer and the Equator and is characterised by three different climatic zones, which are informed by the topographic elevation; the Kolla- tropical zone region below 1830 m ASL, the Woina Dega- subtropical zone that includes the highland areas between 1830 and 2440 m ASL, and the Dega- cool zone that includes areas with an elevation above 2440 m ASL (Figure S3a). The average annual rainfall for the capital, Addis Ababa is 1216 mm y^{-1}, and most of the rainfall falls between June and September (summer), where in the dry season between December and February there is very little rainfall. Ethiopia has a population of approximately 112.1 million and is the second-most populous country in Africa. Approximately 80% of the population live in rural areas and groundwater provides more than 90% for domestic and industry water supply (Kebede, 2012).

The regional geology of Ethiopia is characterised by uplifting, rifting and volcanism, where much of the mountainous terrain exceeds 3000 m in elevation. Two-thirds of the country is covered by volcanic rocks with the remainder covered by sedimentary and metamorphic rocks (Kebede, 2012) (Figure S3a). Formation of continental and marine sedimentary rocks predate the tectonic activities, whereby the uplifting and enhanced rates of erosion over an extended period has produced strongly fragmented and rugged terrain, deep canyons, buttes and mesas. The high rates of erosion and prominent topographic features have influenced the distribution of groundwater resources and climatic patterns in the country (Kebede, 2012). The major aquifer systems are within the unconsolidated Quaternary sediments, Tertiary-Quaternary volcanic rocks and the consolidated sedimentary rocks. The unconsolidated sediments have the greatest storage, with an effective porosity of 20% compared to the volcanic and sedimentary rocks, which only have a porosity of 1%. The more recent Quaternary sediments cover large parts of the rift valley and low-lying depressions, lake margins and river valleys. Watertables are shallow in these sediments, which are generally less than 100 m deep (frequently less than 30 m) and water quality is extremely variable. The volcanic (basalt) rocks tend to be the main fractured rock aquifers in central Ethiopia, due to their stratigraphic position and proximity to the ground surface. The volcanic aquifers are defined by their depth: shallow (30-100 m), deep (100-250 m) and very deep (>250 m). The consolidated sedimentary rocks are dual porosity aquifers, located in the Mekelle outlier, Blue Nile gorge and the south eastern highlands towards Ogaden.

The four main survey areas where the HPBs were sampled are located within the districts of Ejere (9.0°, 38.38°), Abeshege (8.32°, 37.63°), Sodo (8.22°, 38.51°) and Mecha (11.39°, 37.14°). The average annual rainfall for five nearby climate stations (Addis, Bale Robe, Awassa, Bahar Dar and Jimma) to these districts is 1276 mm y^{-1}. The annual average daily air temperature at these stations is 18.2°C and ranged from to 14 to 22°C, and the average elevation is 1991 m ASL. The Ejere district is located 45 km to the west of Addis Ababa and the majority of the HPBs are located within the volcanic basalt aquifers as well as some boreholes in the unconsolidated Quaternary sedimentary aquifers, which despite being shallow, are high yielding. The Abeshege district is located 150 km to the southwest of Addis Ababa and the HPBs are completed in the highly weathered basalt aquifer, which has moderate to high transmissivity values (2 to 6,000 $m^2\ d^{-1}$). The Sodo district is located 85 km to south-southwest of Addis Ababa and the majority of the HPBs are within a pyroclastic tuff deposit, which tends to have a lower aquifer storage than the other major aquifers and lower transmissivity values (15 to 110 $m^2\ d^{-1}$). The Mecha district is located 35 km to the south-west of the township of Bahar Dar in the Lake Tana basin (350 km to the north of Addis Ababa) and the main productive aquifers are within the fractured and strongly weathered Quaternary basalts, which have transmissivity values between 100 to 200 $m^2\ d^{-1}$ (Kebede et al., 2005).

Uganda

Uganda is in eastern Africa and has a tropical climate, which is characterised by a bimodal wet and dry season where there are heavy rainfalls from March to May and from September to November, whilst between December to February and June to August it is the dry season of little to no rainfall (Figure S3b). The average annual rainfall for the capital city Kampala is 1264 mm y^{-1} and has an elevation of 1196 m ASL. The total population in Uganda is 44.2 million (United Nations Department of Economic and Social Affairs Population Division, 2019), with approximately 77% living in rural areas (United Nations Department of Economic and Social Affairs Population Division, 2018). Most of the rural population relies on groundwater, predominantly from shared boreholes equipped with handpumps.

The regional geology of Uganda is comprised of Archaean lithospheric fragments of gneisses and granulites, welded together, intersected or surrounded by metasedimentary rocks of Proterozoic age. The country forms a part of the north-eastern corner of the proto-Congo Craton, composed of several Archaean nuclei and Paleoproterozoic mobile belts (Westerhof et al., 2014) (Figure S3b). The crystalline basement rocks, which constitute 90% of the land area, are covered by a thick layer of weathered saprolite material (Taylor and Howard, 2000; Taylor and Howard, 1998). The major aquifer systems are within the weathered (saprolite) and fractured Precambrian crystalline basement rocks, which typically have low storage and transmissivity values (0.1 to 30 $m^2 d^{-1}$) (Tindimugaya, 2008). These saprolite and fractured bedrock aquifers are the most widely used for shallow boreholes with variable yields between 0.1 to 3 L s^{-1} (Taylor et al., 2003). More productive and higher yielding supplies (in excess of 5 L s^{-1}) are possible in some areas where the bedrock is highly fractured or associated with spatially limited alluvial/fluvial sediments and paleochannel deposits (Maurice et al., 2019).

The sampled HPBs within Uganda were clustered together in three survey areas: the first survey, 60 km to the north of the capital city, Kampala in the Luwero district (0.83°, 32.51°) of Central Uganda, the second survey in Northern Uganda in the Oyam district (2.44°, 32.52°) (45 km to the northwest of the township of Lira), and the third survey area in Eastern Uganda in the districts of Kumi (1.59°, 33.95°) and Budaka (1.14°, 33.95°). The average rainfall for four nearby climate stations (Kampala, Masindi, Lira and Soroti) to the surveyed districts is 1291 mm y^{-1}. The annual average daily air temperature at these stations is 23°C and ranged from to 21.2 to 25.3°C, and the average elevation is 1184 m ASL.

The geology in the survey area in Northern Uganda (Lira and Oyam) are underlain by gneiss, amphibolite and variable gneissic granitoids, in Eastern Uganda (Kumi and Budaka) variable gneissic granitoids and mica gneiss, and Central Uganda (Luwero) comprised of granite and granite gneiss (Westerhof et al., 2014). In each of these survey areas, the HPBs are predominantly completed in the fractured rock aquifers, which are highly weathered and have low transmissivity values (0.02 to 95 $m^2 d^{-1}$).

Malawi

Malawi is located in southeast Africa and has a sub-tropical climate characterised by a wet season from November to March and dry season from April to October when there is very little to no rainfall (Figure S3c). The average annual rainfall is 860 mm y^{-1} for Lilongwe, where the elevation is 1050 MASL. Malawi has a total population of approximately 18.6 million (United Nations Department of Economic and Social Affairs Population Division, 2019), with 83% of the population living in rural areas (United Nations Department of Economic and Social Affairs Population Division, 2018). Malawi is one of many water-stressed countries in Africa, and its rural population is heavily dependent on groundwater as a potable water source (Mapoma and Xie, 2014).

Malawi is positioned at the southern end of one part of the East Africa Rift system, which strongly influences many of the topographic, climatic, hydrological and geological features that can be defined by four regions: (1) the plateau, (2) upland, (3) rift valley escarpment, and (4) rift valley plains. The geology is defined by ancient one-billion-year-old crystalline basement rock, which has been metamorphosed and intruded by igneous rocks during several orogeny mountain building events (Schlueter, 2006). During the Permian era a large and extensive rift system opened and was infilled with sequences of sandstone, mudstone and marl sediments from the Karoo subgroup. These sediments were subsequently down faulted from the late Mesozoic through the Cenozoic, which included the East Africa Rift system and the formation of Lake Malawi and the Shire River.

The lower permeability crystalline basement rocks (0.2 to 1.8 m d^{-1}) provide good quality water (EC < 750 $\mu S\ cm^{-1}$) across most of the country and is the main fractured rock aquifer system (Smith-Carington and Chilton, 1983). There are some areas in the Shire Valley and Bwanje Valley where the basement rock aquifer water quality is poor (EC >4000 $\mu S\ cm^{-1}$) due to evaporite deposits. Shallow aquifers up to 30 metres thick in the unconsolidated weathered basement rock are also found, particularly in plateaus that have considerable depth. More recent unconsolidated alluvial and lakeshore sediments also provide important shallow groundwater resources where the watertable is less than 10 metres depth but water quality is variable as a result of the high level of mineralisation (Figure S3c).

The HPBs that were sampled were located in three survey areas: one in the district of Lilongwe-central region (-13.97°, 33.79°), one in Balaka and Machinga districts- southern region (-14.95°, 35.25°) and one in Nkhotakota-northern region nearby Lake Malawi (-13.04°, 34.08°). The closest climate stations to the survey areas are Lilongwe, Kasungu and Balaka where the average annual rainfall is 884 mm y^{-1}, the average daily air temperature is 22.4°C and ranged from to 16.1 to 26.8°C, and the average elevation at these stations is 913 m ASL.

The geology of the survey area in the northern region is characterised by metamorphosed sandstone units, whilst in the central region it is comprised of basalts, granites and gneisses. In the southern districts of Balaka and Machinga, there is a sequence of sandstone units of the Karoo Subgroup overlying the deeper crystalline igneous rocks (granites, gneisses). Both the sandstone and igneous rocks in the survey areas are fractured rock aquifers, which have transmissivity values from 0.16 to 544 $m^2\ d^{-1}$.

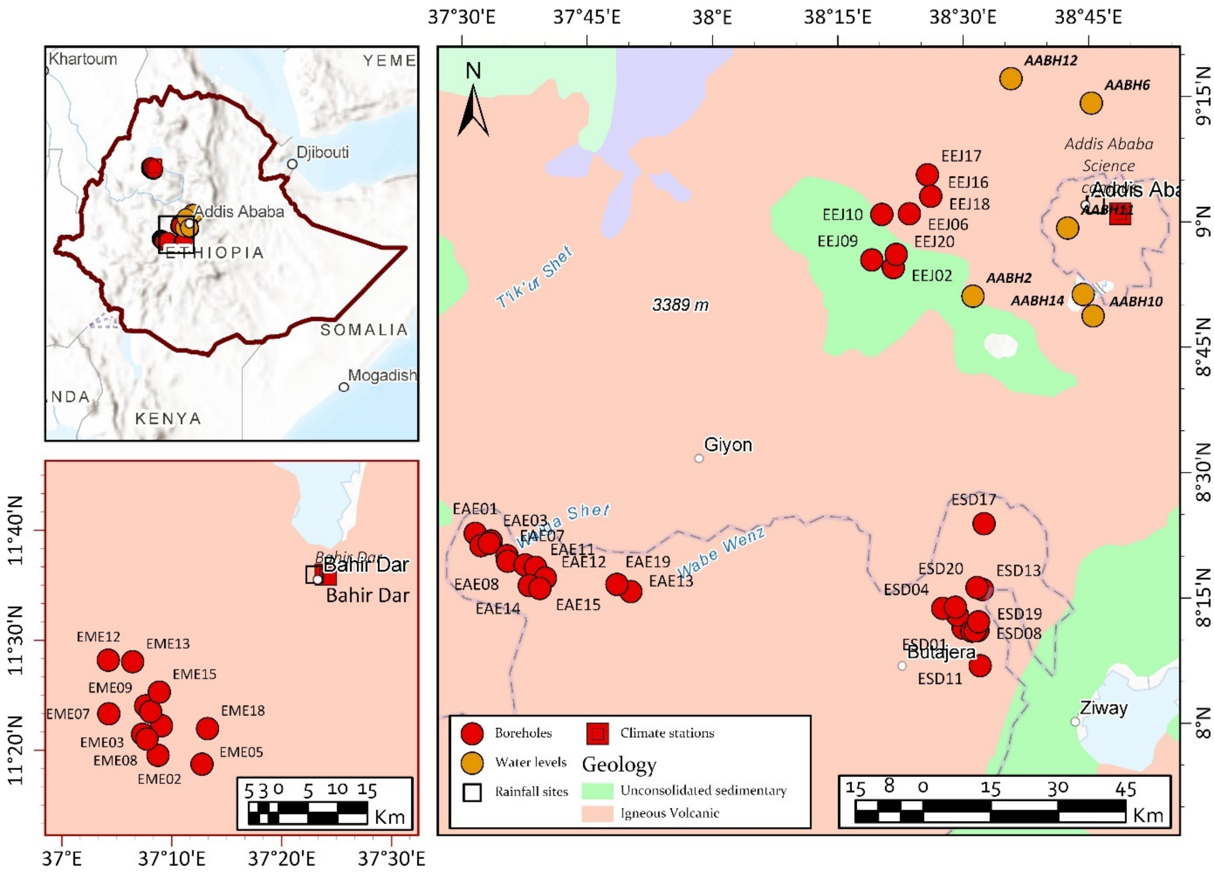

Figure S1. Location maps of Ethiopia. Maps show the locations of the groundwater hand pumped boreholes that were sampled as part of survey 2, location of the rainfall collector sites, boreholes where the water levels were monitored with pressure transducer dataloggers and nearby climate stations with long-term average air temperature and rainfall data. The regional geology are also shown (Ó Dochartaigh, 2019).

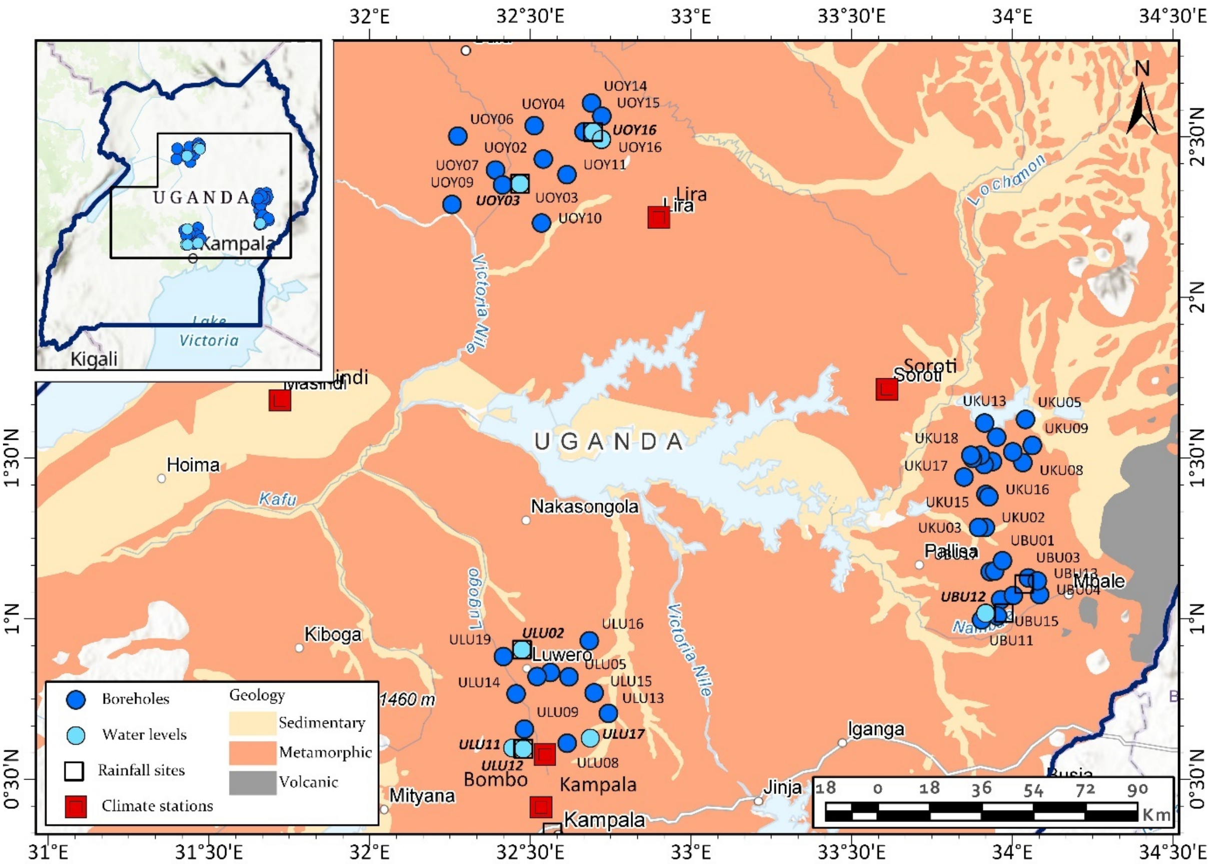

Figure S2. Location maps of Uganda. Maps show the locations of the groundwater hand pumped boreholes that were sampled as part of survey 2, location of the rainfall collector sites, boreholes where the water levels were monitored with pressure transducer dataloggers and nearby climate stations with long-term average air temperature and rainfall data. The regional geology are also shown (Ó Dochartaigh, 2019).

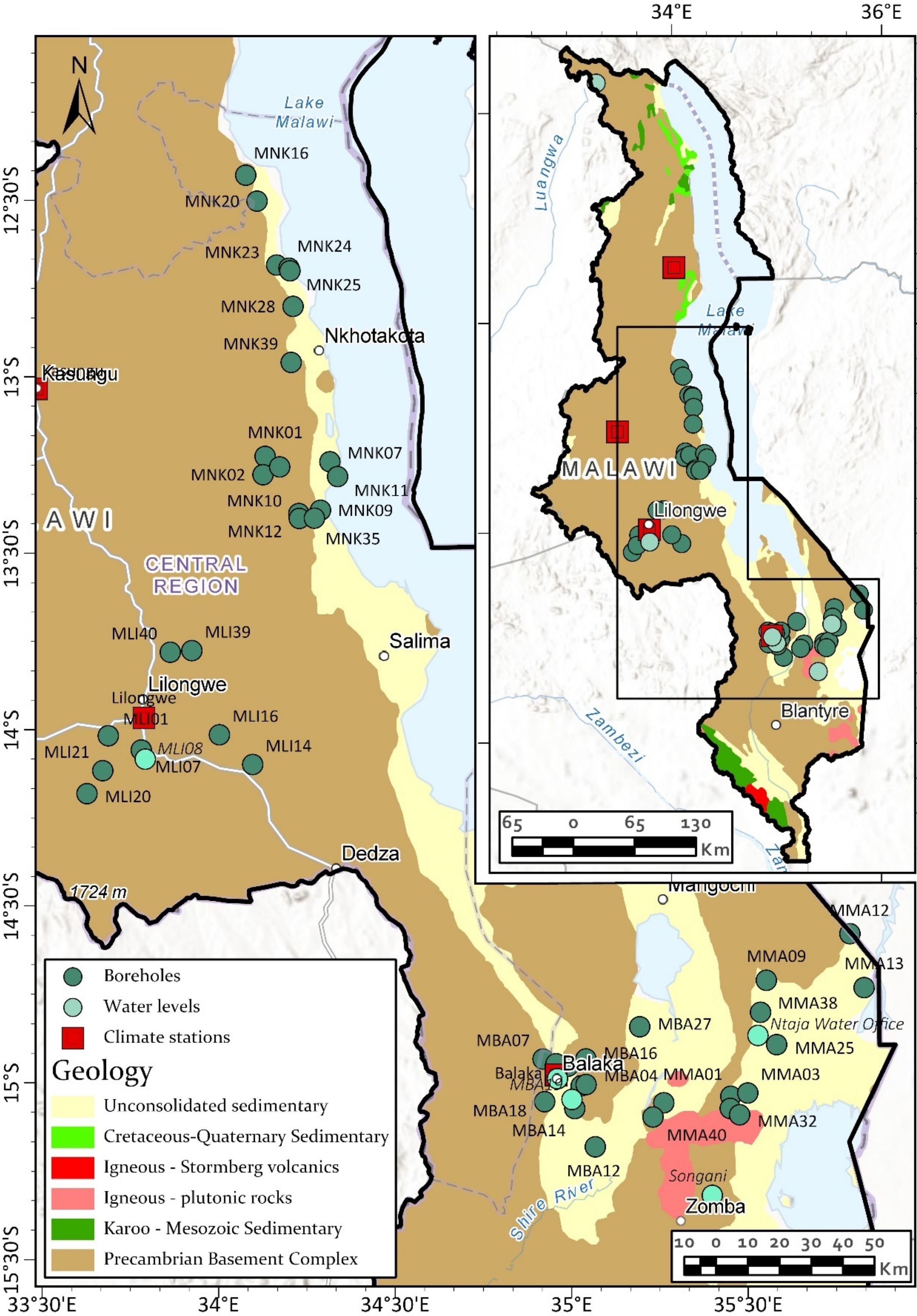

Figure S3. Location maps of Malawi. Maps show the locations of the groundwater hand pumped boreholes that were sampled as part of survey 2, location of the rainfall collector sites, boreholes where the water levels were monitored with pressure transducer dataloggers and nearby climate stations with long-term average air temperature and rainfall data. The regional geology are also shown (Ó Dochartaigh, 2019).

Atmospheric concentrations of CFC-11 and CFC-12 increased in the atmosphere after the 1950s, to peak in concentration between 1994 (CFC-11) and 2003 (CFC-12). Since that time and until 2017 (time of sampling), concentrations have decreased between 3 and 13 %, respectively. In contrast, atmospheric concentrations of SF_6 are still increasing due to its continued release from industrial applications and its stability (Maiss and Brenninkmeijer, 1998) (Figure S4).

Interpretation of CFC and SF_6 concentrations in terms of groundwater residence times is complicated in some environments. Their concentration in groundwater is dependent upon the atmospheric concentration, and on the water temperature at the time of groundwater recharge (i.e. the solubility of CFCs and SF_6 decreases as temperature increases, and hence so does their concentration in groundwater for a given atmospheric concentration). For SF_6, in situ production can occur in some geological formations (Busenberg and Plummer, 2000; von Rohden et al., 2010), resulting in concentrations that are above those that would be expected based on atmospheric concentrations. SF_6 is also subject to contamination due to excess air in recharge (Heaton and Vogel, 1981) or air contamination during borehole drilling and development (Poulsen et al., 2020). CFCs can degrade in anaerobic groundwater, with typical degradation rates for CFC-11 greatly exceeding rates for CFC-12 (Cook et al., 1995; Sebol et al., 2007). Because these processes affect the different CFCs and SF_6 to differing extents, their importance can often be determined from a comparison of tracer concentrations.

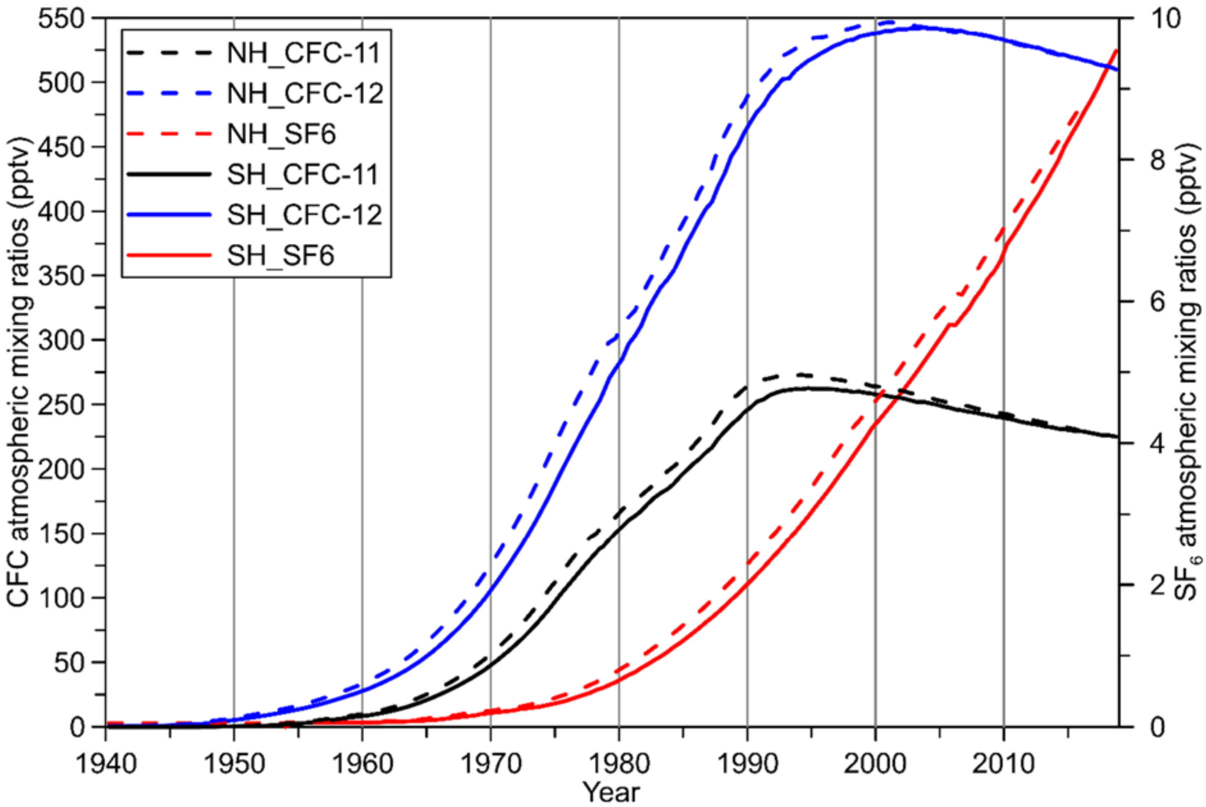

Figure S4. Northern and Southern Hemisphere atmospheric concentrations of CFC-11, CFC-12 and SF_6 using the combined dataset from the NOAA/ESRL Global Monitoring Division available through the National Oceanic and Atmospheric Administration Halocarbons and other Atmospheric Trace Species Group (HATS) database (NOAA, 2019).

SAMPLING AND LABORATORY ANALYSIS

The 150 HPBs that were selected as part of Survey 2 (conducted in 2017 and 2018) for more detailed and comprehensive analysis of borehole construction, water quality and groundwater sampling (Kebede et al., 2019; Mwathunga et al., 2019; Owor et al., 2019) (Table S1) were based upon a detailed site selection criterion to capture the countries' climate, terrain, elevation, soil type, geology, aquifer systems, land use and social-economic factors.

CFCs and SF6 were measured by gas chromatography with an electron capture detector after pre-concentration by cryogenic methods according to Oster et al. (1996) and Busenberg and Plummer (2000), respectively at the British Geological Survey Wallingford, Oxfordshire, UK. The detection limit for both CFCs in water is approximately 1.2 pg kg^{-1} and SF6 is 14 fg kg^{-1}. Corresponding analytical errors in apparent CFC ages are approximately ± 2 years for ages less than 20 years, increasing to ± 4 years for ages of 30 to 50 years. Southern Hemisphere atmospheric concentrations of CFCs and SF6 was sourced from the National Oceanic and Atmospheric Administration (NOAA) Halocarbons and other Atmospheric Trace Species (HATS) group database (NOAA, 2019) (Northern Hemisphere atmospheric concentrations differ by about 5%; Figure S4). The pre-1975 atmospheric data were reconstructed from production and release data tabulated by the Chemical Manufacturers Association. The average recharge temperature for the samples was approximated based on the annual average atmospheric temperature from available meteorological monitoring stations. Calculated recharge rates using Equation 1 (main text) assumed porosity values that ranges from 4 to 8%, 6 to 10%, and 8 to 12% for Ethiopia, Uganda and Malawi, respectively (refer to study site descriptions).

All stable water isotope compositions for the groundwater samples were measured using a Picarro L2130-i Cavity Ring Mass Spectrometer at Flinders University in Adelaide, South Australia. The results are reported as a deviation from Vienna Standard Mean Ocean Water (VSMOW) in per mil (‰) difference using delta (δ) notation. The analytical precision for $\delta^{18}O$ and $\delta^{2}H$ is ±0.025 ‰ and ±0.1 ‰, respectively.

Groundwater samples for major and trace elements were filtered using a 0.45-micron filter, collected in 60 mL HDPE plastic bottles, cation samples were acidified with nitric acid (1 % by volume HNO3). Analysis was performed on an Agilent 7500cx series inductively-coupled plasma mass spectrometer (ICP-MS) for major cations and trace metals, and a Dionex ICS-5000 Ion Chromatograph system for anions at the British Geological Survey Keyworth Environmental Science Centre, UK. Instruments were calibrated at the beginning and end of every analytical run using QC standards (ISO 17034 compliant) and uncertainty associated with measurements away from the detection limits is ±10 %. The ion charge balance error based on the major cation and anion analytes measured for each sample were better than ±5 %.

Rainfall and rainfall chloride values were used to estimate recharge according to the CMB technique (i.e. P and C_p) and were based on the data collected from selected sites. These sites were equipped with monthly rainfall collectors to measure rainfall amount and chloride concentration (Table S4). The locations of the rainfall collector sites are shown in Figure S1, S2 and S3, within the survey districts where the sampling of the HPBs was undertaken. There were three sites in Ethiopia, eight sites in Uganda and five sites in Malawi, which all had at least one year of data.

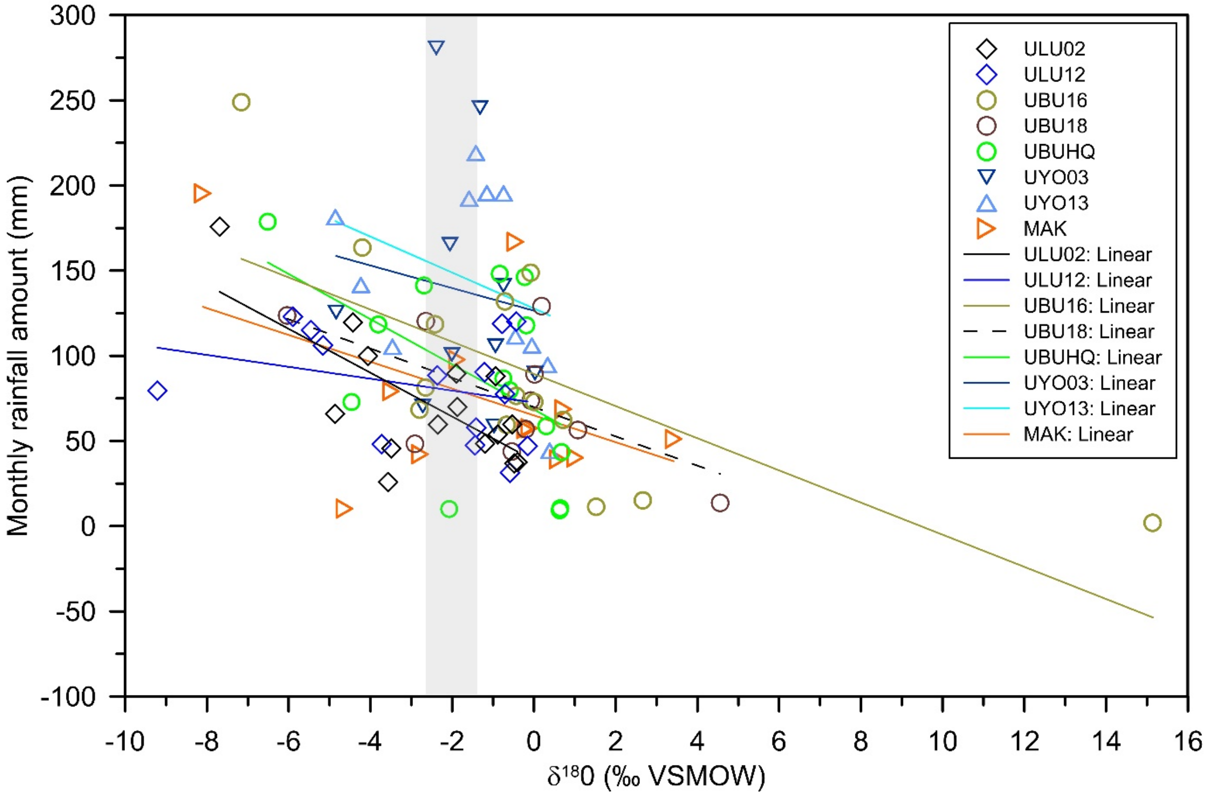

Figure S5. Monthly rainfall volume versus measured $\delta^{18}O$ for the eight rainfall collectors installed in Uganda. Shaded area represents the range in groundwater $\delta^{18}O$ values. Linear trend lines are also shown for each site.

Table S1. Environmental tracer and water chemistry data of the sampled handpump boreholes in Ethiopia. nm = not measured.

WP ID	Long	Lat	Elevation (mASL)	Date drilled	Well depth (m)	Mid-screen (m)	1/2 screen length (m)	Date sampled	SWL (mbgl)	SWL (m below top of screen)	Temp (°C)	DO (mgL^{-1})	pH	EC ($microSiemenscm^{-1}$)	Chloride (mgL^{-1})	Nitrate (mgL^{-1})	E. coli ($MPN100mL^{-1}$)	CFC-11 ($pgkg^{-1}$)	CFC-12 ($pgkg^{-1}$)	SF6 ($fgkg^{-1}$)
EAE01	37.53	8.38	1548	2012	70.30	64.05	6.25	6/03/2017	21.55	36.25	25.8	1.3	7.0	457.7	4.2	7.1	0.0	122.9	64.7	138.1
EAE02	37.54	8.35	1513	1977	44.86	41.43	3.43	6/01/2017	12.60	25.40	24.2	1.1	7.0	431.5	6.8	0.6	0.0	76.0	115.2	257.5
EAE03	37.56	8.36	1562	1995	76.00	64.05	6.25	6/07/2017	53.01	4.79	26.30	0.1	7.0	689.6	48.3	0.3	2.6	319.5	156.1	31.1
EAE04	37.55	8.36	1580	1989	60.78	60.25	0.53	6/05/2017	49.30	10.42	25.70	0.2	7.1	455.4	21.0	0.6	4.7	70.6	69.4	58.5
EAE07	37.59	8.33	1531	1995	43.50	40.20	3.30	1/06/2017	24.28	12.62	25.50	0.6	6.9	404.4	17.1	34.9	1.5	120.5	76.2	43.7
EAE08	37.59	8.32	1527	1994	47.13	44.33	2.81	7/07/2017	20.00	21.52	26.20	0.4	6.9	947.0	184.7	201.3	13.6	431.9	79.9	28.6
EAE10	37.63	8.32	1614	1999	84.30	80.25	4.06	7/05/2017	62.20	13.99	27.10	0.1	8.8	353.1	41.3	0.3	13.6	300.0	103.0	35.9
EAE11	37.65	8.31	1630	2000	51.45	46.17	5.28	1/06/2017	12.21	28.68	25.80	2.6	7.7	349.4	31.5	0.5	0.0	58.8	72.9	275.1
EAE12	37.67	8.29	1689	2004	76.70	66.53	10.18	1/06/2017	23.11	33.24	25.40	1.3	7.3	339.5	0.9	0.1	13.6	153.6	97.1	90.6
EAE13	37.84	8.26	1639	2003	73.66	66.97	6.69	1/06/2017	60.21	0.07	28.40	4.7	7.1	633.9	19.6	12.8	3.4	527.5	236.8	82.6
EAE14	37.63	8.27	1605	2008	76.88	73.59	3.29	7/03/2017	58.05	12.25	26.80	0.1	6.7	440.7	38.0	0.3	0.0	59.5	22.9	159.0
EAE15	37.66	8.27	1587	2008	83.42	70.41	13.01	6/09/2017	72.63	-15.23	nm	nm	nm	nm	nm	nm	nm	nm	nm	nm
EAE19	37.81	8.28	1865	2010	63.69	54.73	8.97	6/09/2017	25.25	20.51	24.70	0.5	6.5	129.6	0.6	0.4	0.0	35.1	25.2	78.8
EEJ02	38.36	8.91	2051	2010	49.50	32.15	17.35	1/09/2017	8.14	6.66	21.80	0.1	7.3	340.0	2.6	0.1	0.0	3.2	7.9	0.0
EEJ06	38.39	9.02	2130	2013	62.67	40.92	21.75	1/09/2017	3.56	15.61	21.80	0.2	6.7	676.0	8.2	0.2	0.0	314.4	151.3	116.2
EEJ09	38.32	8.92	2074	2002	35.60	31.08	4.53	1/09/2017	5.80	20.75	22.80	0.1	7.2	327.5	4.6	0.0	0.0	12.7	23.6	30.0
EEJ10	38.34	9.02	2152	2007	46.88	32.11	14.78	1/09/2017	7.15	10.18	23.40	0.1	7.4	253.1	4.2	0.0	0.0	135.0	103.1	150.6
EEJ16	38.44	9.05	2600	2013	62.66	46.32	16.35	1/09/2017	15.08	14.89	18.00	2.8	7.1	162.4	3.7	14.0	0.0	438.4	319.3	200.8
EEJ17	38.43	9.09	2532	2003	47.35	35.50	11.86	1/09/2017	26.65	-3.01	19.10	0.9	7.4	103.9	0.9	1.4	0.0	126.2	112.5	114.2
EEJ18	38.44	9.05	2395	2016	51.50	40.05	11.45	4/12/2017	39.20	-10.60	21.70	2.3	6.4	273.5	3.5	6.0	0.0	213.5	178.8	0.0
EEJ20	38.37	8.94	2095	2003	53.39	43.70	9.70	4/11/2017	32.40	1.60	21.90	0.4	6.4	1028.0	78.0	104.6	0.0	235.7	203.1	0.0
EME01	37.15	11.37	2033	2007	21.75	20.15	1.61	9/08/2017	10.26	8.28	22.10	2.8	6.3	76.8	0.5	2.3	4.7	523.1	192.6	384.0
EME02	37.15	11.33	2029	2007	25.85	20.99	4.87	1/08/2017	10.76	5.36	21.50	2.7	6.6	95.3	0.5	2.3	4.7	357.9	133.0	254.5
EME03	37.12	11.36	2010	2007	53.26	44.25	9.01	1/08/2017	17.47	17.77	22.10	1.0	6.2	101.0	2.9	9.7	0.0	546.6	225.2	138.3
EME05	37.21	11.31	2065	2007	49.00	43.71	5.30	7/08/2017	9.31	29.10	21.90	0.9	6.4	133.5	2.0	3.7	nm	378.8	157.8	41.2
EME07	37.07	11.39	1938	2007	61.34	37.49	23.86	1/08/2017	2.41	11.22	22.60	0.1	6.0	69.0	4.6	2.6	48.3	434.2	210.5	129.3
EME08	37.13	11.35	2016	2007	49.02	35.65	13.38	1/08/2017	16.12	6.15	22.30	0.7	5.9	75.2	0.5	5.0	0.0	626.5	211.3	94.0
EME09	37.13	11.40	1998	2007	51.42	31.50	19.92	1/08/2017	6.55	5.03	22.60	0.3	6.2	102.5	4.0	0.2	nm	215.0	122.9	104.8
EME10	37.13	11.39	2018	2010	30.00	25.17	4.84	14/08/2017	24.35	-4.02	22.20	3.9	6.5	124.0	0.5	1.2	0.0	555.8	220.9	383.3

EME12	37.07	11.47	1914	2007	42.50	27.21	15.30	4/08/2017	4.96	6.95	22.20	0.6	5.5	50.5	10.1	0.8	1.2	545.8	253.6	173.4
EME13	37.11	11.47	1917	2007	50.00	42.70	7.30	2/08/2017	23.17	12.23	23.10	2.5	6.1	83.4	2.5	3.8	nm	430.6	173.2	166.6
EME15	37.15	11.42	2005	2007	50.32	32.48	17.84	11/08/2017	11.42	3.22	22.20	2.7	5.9	85.0	0.9	2.3	3.4	426.4	140.4	249.7
EME18	37.22	11.37	2047	2007	54.45	39.04	15.42	1/08/2017	8.95	14.67	22.30	0.6	6.0	75.8	2.2	9.7	48.5	219.3	170.5	124.7
ESD01	38.50	8.19	1865	2004	25.30	22.65	2.65	1/08/2017	10.32	9.68	24.1	0.1	6.6	128.4	7.7	2.2	0.0	47.3	87.8	330.7
ESD03	38.49	8.22	1896	2004	38.05	29.94	8.12	5/08/2017	19.12	2.70	23.60	0.9	6.4	128.6	2.8	0.3	0.0	468.8	249.1	146.7
ESD04	38.46	8.23	1969	2009	68.60	56.38	12.22	5/03/2017	21.00	23.16	20.70	1.0	6.7	122.2	3.6	6.7	13.6	318.3	212.4	154.5
ESD08	38.53	8.18	1866	2010	62.00	53.11	8.89	5/09/2017	40.62	3.60	28.40	1.5	7.1	246.9	1.5	0.0	13.6	435.9	204.8	166.7
ESD09	38.52	8.18	1851	2004	35.71	32.24	3.47	1/10/2017	15.00	13.77	24.10	0.3	6.9	320.2	8.9	0.2	0.0	193.8	104.2	115.8
ESD10	38.52	8.18	1859	2004	51.50	45.92	5.59	5/11/2017	23.56	16.77	24.40	2.6	6.7	274.3	3.7	3.5	0.0	831.3	276.9	119.8
ESD11	38.53	8.11	1853	2003	42.94	36.47	6.47	1/10/2017	20.38	9.62	25.80	0.3	7.1	411.0	11.4	0.2	0.0	474.9	282.3	128.5
ESD13	38.54	8.27	2084	1998	18.60	18.18	0.43	5/02/2017	15.01	2.74	23.30	1.4	7.0	167.8	1.4	0.0	0.0	nm	nm	nm
ESD16	38.49	8.23	1906	2003	43.50	41.05	2.46	1/03/2017	22.20	16.39	24.3	1.1	6.8	130.6	2.9	2.7	nm	91.2	63.0	278.8
ESD17	38.54	8.40	2521	2012	47.00	44.91	2.10	1/03/2017	38.81	4.00	21.1	2.4	6.7	91.7	1.1	3.8	0.0	604.2	204.3	438.7
ESD19	38.53	8.20	1896	2010	80.00	68.41	11.59	5/05/2017	52.01	4.81	26.70	3.4	6.6	149.6	1.0	0.0	nm	43.2	48.4	59.9
ESD20	38.53	8.27	1954	2011	75.10	70.30	4.80	1/03/2017	40.75	24.75	25.40	1.8	6.9	199.2	1.2	0.0	0.0	577.4	215.1	175.9

Table S2. Environmental tracer and water chemistry data of the sampled handpump boreholes in Uganda. nm = not measured.

WP ID	Long	Lat	Elevation (mASL)	Date drilled	Well depth (m)	Mid-screen (m)	1/2 screen length (m)	Date sampled	SWL (mbgl)	SWL (m below top of screen)	Temp (°C)	DO (mgL^{-1})	pH	EC (micro $Siemenscm^{-1}$)	Chloride (mgL^{-1})	Nitrate (mgL^{-1})	E. coli ($MPN100mL^{-1}$)	CFC-11 ($pgkg^{-1}$)	CFC-12 ($pgkg^{-1}$)	SF6 ($fgkg^{-1}$)
UBU01	33.97	1.18	1081	2015	48.45	43.17	5.28	20-Nov-17	7.68	30.21	30.1	0.9	6.1	80.5	4.7	0.0	0.1	135.3	79.8	34.9
UBU03	34.05	1.13	1120	2013	68.12	50.64	17.48	13-Nov-17	5.18	27.98	26.7	1.0	6.0	105.1	22.1	0.4	1.2	163.5	79.9	33.1
UBU04	34.09	1.07	1121	2015	55.34	43.62	11.72	22-Nov-17	5.36	26.55	28.2	0.7	6.8	138.6	2.4	3.7	48.3	138.4	116.5	74.5
UBU05	33.95	1.15	1138	2011	50.95	44.52	6.43	17-Nov-17	10.54	27.55	26.8	1.6	5.7	18.3	18.6	4.5	0.1	298.4	138.4	53.6
UBU08	33.96	1.06	1126	2015	54.49	51.40	3.10	8-Nov-17	9.95	38.35	26.3	0.8	6.3	291.5	74.8	13.3	1.5	121.2	100.4	37.7
UBU10	34.00	1.07	1134	2006	30.42	26.69	3.73	9-Nov-17	6.04	16.92	27.8	1.0	5.9	184.7	21.6	59.0	13.6	269.2	168.1	1650.5
UBU11	33.91	1.00	1089	2000	59.55	50.14	9.41	6-Nov-17	10.43	30.30	27.6	3.3	6.1	235.6	49.9	15.3	9435.1	172.3	121.0	845.8
UBU12	33.92	1.02	1143	2012	101.44	63.07	38.37	3-Nov-17	11.70	13.00	27.9	0.9	5.5	156.7	30.2	70.3	4.7	216.1	180.0	168.2
UBU13	34.08	1.12	1132	2012	38.93	29.33	9.60	27-Nov-17	8.10	11.64	28.1	2.4	5.7	74.1	13.7	17.9	48.3	312.0	212.4	873.4
UBU15	33.96	1.01	1133	1960	86.62	55.76	30.86	24-Nov-17	9.10	15.80	27.1	0.6	6.2	144.2	12.6	6.7	0.1	144.9	152.1	88.9
UBU17	33.93	1.15	1138	2003	58.74	44.97	13.77	15-Nov-17	10.08	21.12	29.1	5.0	6.2	101.9	3.8	0.4	13.6	279.2	180.4	114.6
UKU02	33.92	1.28	1082	2015	26.00	24.49	1.52	22-Sep-17	5.75	17.22	27.8	4.0	5.7	54.3	2.2	13.3	1.5	793.3	420.2	294.2
UKU03	33.90	1.28	1065	2013	62.00	49.88	12.13	27-Sep-17	6.37	31.38	29.4	0.9	6.0	83.2	0.9	2.1	3.4	239.6	109.6	362.8
UKU05	34.04	1.62	1041	2008	45.30	40.73	4.58	10-Oct-17	10.07	26.08	31.1	1.7	6.8	336.9	32.8	4.4	0.1	84.2	59.0	173.8
UKU08	34.03	1.49	1076	1998	71.16	37.18	33.99	12-Oct-17	23.09	-19.90	31.5	2.4	6.8	302.1	8.2	0.5	9.6	87.1	70.2	3105.6
UKU09	34.06	1.54	1071	1962	38.05	29.50	8.55	14-Oct-17	13.07	7.88	29.8	1.1	6.5	220.5	6.9	0.1	1.5	44.4	41.0	63.6
UKU10	33.94	1.49	1150	2010	89.10	62.00	27.10	6-Sep-17	8.15	26.75	28.6	1.4	6.6	204.9	6.6	18.0	0.1	179.2	111.6	81.3
UKU11	34.00	1.52	1074	2015	47.06	35.57	11.50	6-Oct-17	3.11	20.96	31.0	nm	nm	nm	7.9	12.8	13.6	228.3	145.6	159.0
UKU12	33.95	1.57	1047	2011	45.06	41.49	3.58	2-Oct-17	1.48	36.43	29.9	0.4	6.5	317.8	46.6	20.3	1.2	92.1	95.3	369.5
UKU13	33.91	1.61	1053	2009	67.70	58.85	8.85	4-Oct-17	4.10	45.90	30.4	0.8	6.7	724.7	228.0	27.2	3.4	60.4	55.3	71.8
UKU14	33.90	1.51	1139	1960	66.30	47.85	18.45	11-Sep-17	26.80	2.60	32.2	1.5	6.6	264.6	1.3	0.9	13.6	183.1	124.8	97.1
UKU15	33.92	1.39	1104	2010	80.15	56.31	23.85	20-Sep-17	6.26	26.20	30.9	2.0	6.6	160.6	1.1	17.5	13.6	5.1	15.3	17846.2
UKU16	33.93	1.38	1123	1960	50.26	33.38	16.88	29-Sep-17	5.44	11.06	28.7	0.4	6.7	287.7	6.1	18.5	100.0	5.9	10.9	38715.4
UKU17	33.85	1.44	1115	1987	75.20	62.60	12.60	18-Sep-17	18.53	31.47	29.9	4.4	6.1	96.7	2.6	31.1	0.1	144.9	102.9	2729.9
UKU18	33.87	1.51	1139	2003	80.20	56.37	23.84	13-Sep-17	10.24	22.29	29.1	0.3	6.3	174.5	1.0	0.1	0.1	27.7	19.4	1211.0
UKU19	33.88	1.50	1147	2006	62.10	40.34	21.76	15-Sep-17	22.81	-4.23	32.3	3.9	6.4	190.9	2.5	0.1	48.3	176.3	141.0	2491.5
UKU20	33.91	1.48	1117	2012	26.90	25.45	1.45	8-Sep-17	3.24	20.76	28.8	0.4	6.3	130.5	2.8	0.3	0.1	86.9	68.9	397.7
ULU03	32.52	0.82	1095	1987	37.60	33.30	4.30	22-Jun-17	14.40	14.60	25.7	0.9	6.1	157.3	6.4	6.2	2.4	565.9	221.8	404.9
ULU04	32.56	0.83	1095	1995	38.60	34.30	4.30	20-Jun-17	13.41	16.59	24.4	1.8	5.9	149.3	22.6	0.1	9.6	178.3	87.9	409.3
ULU05	32.62	0.82	1071	1990	46.10	41.05	5.05	10-Jul-17	17.92	18.08	25.8	2.1	6.2	181.3	19.6	0.1	0.1	175.7	75.6	43114.8
ULU08	32.61	0.61	1143	2013	63.80	46.61	17.20	26-Jun-17	19.14	10.27	24.6	6.4	6.5	128.1	15.1	17.9	nm	346.1	161.4	612.6

ULU09	32.48	0.66	1172	1987	52.00	41.00	11.00	7-Jul-17	16.03	13.97	23.9	0.5	6.3	155.8	6.7	3.1	48.3	213.4	138.7	309.9
ULU13	32.74	0.70	1063	1940	25.65	25.53	0.13	24-Jun-17	20.03	5.37	28.3	2.2	6.1	134.5	6.6	9.9	13.6	530.0	234.9	1572.6
ULU14	32.46	0.77	1118	1994	37.20	26.90	10.30	30-Jun-07	17.02	-0.42	27.0	2.0	6.4	202.9	4.7	4.4		379.7	151.3	625.1
ULU15	32.70	0.77	1068	2000	47.00	28.80	18.20	3-Jul-17	20.14	-9.54	23.9	2.7	6.3	193.4	5.2	1.0	0.1	85.8	29.0	12476.2
ULU16	32.68	0.93	1066	1995	85.70	68.90	16.80	5-Jul-17	26.53	25.58	23.8	3.4	6.4	242.1	39.7	16.4	nm	149.6	82.1	389.2
ULU19	32.42	0.88	1076	1987	50.30	40.15	10.15	28-Jun-17	13.81	16.19	27.7	1.7	5.9	1405.0	153.0	0.6	1.2	125.6	90.0	376.2
UOY02	32.54	2.43	1048	2010	24.70	23.35	1.35	4-Aug-17	4.06	17.94	27.2	0.4	6.4	115.2	0.2	0.1	32.6	50.4	60.3	37.7
UOY03	32.47	2.35	1053	2012	37.20	36.85	0.35	11-Jun-17	8.32	28.18	26.6	0.6	6.4	112.0	0.7	0.1	13.6	107.9	90.6	128.9
UOY04	32.51	2.54	1076	2011	55.10	51.05	4.05	7-Aug-17	8.03	38.97	26.8	0.5	5.9	85.3	0.6	0.0	0.1	40.9	29.7	2014.1
UOY06	32.27	2.50	1073	1994	71.00	52.45	18.55	31-Jul-17	9.77	24.13	25.6	3.4	6.1	106.4	0.2	0.0	1.2	82.2	140.7	229.5
UOY07	32.39	2.40	1060	2012	53.50	26.75	26.75	20-Jul-17	12.36	-12.36	25.7	5.2	6.1	106.9	0.4	18.8	0.1	74.5	186.8	134.2
UOY08	32.41	2.35	1041	2011	58.40	51.15	7.25	22-Jul-17	10.96	32.94	27.3	2.4	7.0	240.7	16.8	0.1	1.0	41.0	63.1	79.7
UOY09	32.26	2.29	1068	2012	46.10	34.20	11.90	24-Jul-17	9.72	12.58	25.8	0.4	5.9	109.2	0.7	0.0	1.2	72.2	72.6	47.2
UOY10	32.53	2.23	1041	2012	41.10	33.85	7.25	28-Jul-17	8.34	18.26	27.6	2.6	6.1	104.2	7.0	14.5	nm	218.8	186.5	486.8
UOY11	32.61	2.38	1082	1960	69.00	47.55	21.45	2-Aug-17	7.10	19.00	26.2	0.7	6.0	91.1	1.1	6.8	3.4	245.1	139.4	175.2
UOY14	32.69	2.61	1062	2015	59.65	41.78	17.88	14-Aug-17	6.05	17.85	26.9	4.7	6.2	100.1	0.2	17.1	0.1	218.0	146.0	285.4
UOY15	32.72	2.57	1074	2011	74.60	53.15	21.45	16-Aug-17	8.61	23.09	27.3	1.2	6.4	191.9	2.9	3.0	0.1	44.8	47.3	142.4
UOY16	32.72	2.49	1108	2015	35.85	25.73	10.13	11-Aug-17	1.51	14.09	26.8	0.7	6.1	101.1	1.9	0.0	0.1	49.5	34.1	84.3
UOY19	32.67	2.52	1106	2011	38.60	28.30	10.30	9-Aug-17	13.41	4.59	28.6	1.2	6.1	114.7	4.4	4.6	0.1	93.8	95.4	109.7

Table S3. Environmental tracer and water chemistry data of the sampled handpump boreholes in Malawi. nm = not measured.

WP ID	Long	Lat	Elevation (mASL)	Date drilled	Well depth (m)	Mid-screen (m)	1/2 screen length (m)	Date sampled	SWL (mbgl)	SWL (m below top of screen)	Temp (°C)	DO (mgL^{-1})	pH	EC ($microSiemenscm^{-1}$)	Chloride (mgL^{-1})	Nitrate (mgL^{-1})	E. coli ($MPN100 mL^{-1}$)	CFC-11 ($pgkg^{-1}$)	CFC-12 ($pgkg^{-1}$)	SF6 ($fgkg^{-1}$)
MBA02	-14.96	34.96	626	2014	20.35	15.62	4.73	24-Oct-17	12.31	-1.42	29.7	0.2	6.8	2736.0	431.3	6.4	0.0	159.5	59.9	68.6
MBA03	-15.01	35.03	596	1961	18.75	17.55	1.20	17-Nov-17	13.33	3.02	28.8	0.3	6.8	1712.0	48.7	0.6	1.0	22.7	36.5	35.3
MBA04	-15.01	35.04	631	2005	51.42	40.66	10.76	15-Nov-17	26.98	2.92	27.4	0.3	6.7	982.4	15.3	0.3	4.7	242.3	127.8	83.2
MBA07	-14.93	34.92	708	1997	45.27	34.75	10.52	26-Nov-17	18.34	5.89	32.3	4.4	6.5	618.4	6.3	0.2	48.3	1110.0	371.9	164.7
MBA12	-15.18	35.07	508	2009	45.00	26.25	18.76	1-Nov-17	10.60	-3.11	28.6	0.1	6.9	850.8	15.3	0.3	2.4	49.8	48.0	44.9
MBA14	-15.07	35.01	577	2014	59.45	47.90	11.55	3-Nov-17	27.39	8.96	28.7	2.7	6.7	1576.0	118.5	23.6	0.0	95.7	73.1	108.7
MBA16	-14.93	35.04	660	2014	51.78	44.29	7.50	13-Nov-17	23.00	13.79	28.0	1.8	6.5	598.4	7.1	7.9	0.0	60.2	64.9	110.6
MBA17	-14.95	34.99	615	1995	50.22	40.16	10.06	10-Nov-17	8.35	21.76	28.1	3.1	6.8	2589.0	320.1	14.6	0.0	292.2	150.1	139.8
MBA18	-15.05	34.92	628	1980	14.73	11.66	3.07	6-Nov-17	13.27	-4.68	27.7	0.6	6.9	1524.0	46.3	9.4	0.0	60.5	143.6	171.5
MBA27	-14.84	35.19	522	1994	28.52	20.18	8.35	8-Nov-17	10.63	1.20	29.9	0.1	6.6	2939.0	487.9	1.5	0.0	6.4	13.6	0.0
MBA37	-14.95	34.96	642	9999	40.62	32.21	8.42	20-Nov-17	15.15	8.64	27.2	0.0	6.6	672.8	6.6	0.2	1.2	11.3	45.2	0.0
MBA38	-14.95	34.96	646	2012	40.73	27.06	13.67	22-Nov-17	13.37	0.02	25.4	0.0	6.4	309.1	4.9	0.2	0.0	31.9	41.1	0.0
MLI01	-14.02	33.69	1106	2015	46.02	36.46	9.56	28-Feb-18	9.02	17.88	26.3	1.2	6.8	726.7	1.3	0.1	1.1	44.0	26.3	45.8
MLI07	-14.06	33.78	1100	2014	65.80	37.01	28.80	8-Mar-18	9.60	-1.39	25.1	4.2	7.1	689.4	1.2	0.2	0.0	100.5	94.4	111.7
MLI14	-14.10	34.10	1155	1980	30.25	22.91	7.35	13-Mar-18	6.30	9.26	24.6	1.9	6.7	741.4	11.1	0.2	0.0	503.5	169.9	136.7
MLI16	-14.01	34.00	1090	1980	40.90	26.70	14.21	23-Mar-18	5.46	7.03	26.8	0.5	6.8	487.9	2.0	0.2	4.7	261.3	154.1	139.3
MLI20	-14.18	33.63	1119	1996	24.80	17.98	6.82	2-Mar-18	13.43	-2.27	26.4	3.9	6.3	308.8	4.9	26.8	3.4	66.9	87.3	66.3
MLI21	-14.12	33.67	1124	1984	43.80	27.56	16.24	6-Mar-18	12.08	-0.76	31.7	0.7	6.9	1312.0	5.6	17.0	48.3	289.1	211.5	159.8
MLI39	-13.78	33.92	1101	1980	32.25	19.56	12.70	19-Mar-18	7.71	-0.85	25.3	0.3	6.5	963.2	3.1	0.6	0.0	17.8	89.6	46.8
MLI40	-13.78	33.86	1177	1990	17.80	14.48	3.32	21-Mar-18	3.18	7.98	27.2	0.0	6.5	556.1	17.7	15.6	0.0	63.0	103.2	106.8
MMA01	-15.04	35.45	728	1999	31.10	20.97	10.14	29-Sep-17	8.75	2.08	27.1	3.7	6.4	418.6	23.2	0.2	0.0	64.9	44.3	0.0
MMA02	-15.07	35.45	707	2002	33.33	24.67	8.67	25-Sep-17	14.75	1.25	30.6	1.8	5.9	154.1	2.1	0.7	13.6	94.5	180.4	133.7
MMA03	-15.03	35.50	670	1958	25.76	17.91	7.86	22-Sep-17	14.45	-4.40	36.2	1.0	6.2	695.5	4.8	2.0	0.0	671.3	303.3	189.3
MMA09	-14.71	35.55	884	1998	19.50	13.98	5.52	9-Oct-17	7.34	1.12	27.5	0.3	5.7	125.1	5.1	0.0	1.5	293.7	214.0	nm
MMA12	-14.58	35.79	707	2012	44.88	34.22	10.66	6-Oct-17	17.00	6.56	31.3	6.9	7.1	836.1	33.2	0.3	0.0	376.8	168.4	nm

MMA13	-14.73	35.83	635	2000	37.30	32.12	5.19	4-Oct-17	11.72	15.21	30.1	0.7	6.1	223.7	9.4	0.1	0.0	260.1	148.7	179.3
MMA25	-14.89	35.58	688	2001	36.00	26.37	9.63	11-Oct-17	12.10	4.64	26.7	0.1	6.1	276.5	4.8	0.1	0.0	278.3	206.6	168.3
MMA32	-15.09	35.48	662	9999	41.00	34.50	6.51	27-Sep-17	6.06	21.93	27.7	0.0	6.6	311.2	5.5	0.1	0.0	29.7	13.0	0.0
MMA33	-15.06	35.26	496	2014	23.87	18.19	5.68	30-Sep-17	10.22	2.29	29.7	nm	6.4	823.7	nm	nm	nm	15.0	0.0	0.0
MMA38	-14.80	35.54	774	2005	38.35	23.48	14.88	13-Oct-17	9.97	-1.37	27.2	0.4	5.8	201.0	7.7	15.5	1.5	117.1	157.0	121.4
MMA40	-15.10	35.23	525	9999	32.32	21.31	11.01	20-Sep-17	13.12	-2.82	30.9	0.2	7.4	742.1	35.4	1.0	0.0	17.0	52.5	190.1
MNK01	-13.23	34.13	625	2004	42.58	30.85	11.73	12-Dec-17	15.82	3.30	28.0	0.1	6.5	520.5	6.2	0.2	1.5	30.3	35.7	71.4
MNK02	-13.28	34.12	648	9999	21.20	17.18	4.02	4-Dec-17	10.14	3.02	27.7	1.6	5.4	127.8	6.4	0.0	1.0	528.9	207.2	174.5
MNK06	-13.25	34.17	596	9999	27.10	22.79	4.32	7-Dec-17	14.65	3.82	29.4	0.1	5.9	213.5	3.6	0.1	2.6	30.8	99.5	85.5
MNK07	-13.24	34.31	530	9999	42.95	32.75	10.21	15-Feb-18	16.48	6.06	30.3	1.4	6.1	271.1	0.7	0.1	0.0	51.8	68.2	89.8
MNK09	-13.38	34.29	499	2007	40.20	31.82	8.39	18-Jan-18	7.42	16.01	28.7	0.1	6.8	536.9	1.1	0.2	4.7	34.0	19.6	27.9
MNK10	-13.39	34.23	547	1991	31.00	20.53	10.48	24-Jan-18	4.13	5.92	28.1	0.1	6.6	394.0	5.0	0.1	48.3	29.6	72.6	77.6
MNK11	-13.28	34.34	488	2004	43.45	29.93	13.53	26-Jan-18	6.50	9.90	29.1	1.4	6.4	212.9	2.7	0.1	0.0	178.6	185.3	nm
MNK12	-13.40	34.23	552	1992	48.09	38.01	10.08	22-Jan-18	13.70	14.23	28.8	0.3	6.5	711.9	9.0	0.2	0.0	41.5	64.5	nm
MNK16	-12.43	34.08	521	2002	33.10	29.71	3.40	15-Dec-17	23.36	2.95	29.1	4.5	4.7	43.2	1.4	0.0	1.5	303.9	183.3	251.7
MNK20	-12.50	34.11	498	2002	15.80	11.05	4.75	18-Dec-17	13.12	-6.82	28.2	3.8	5.7	155.0	5.8	10.4	4.7	234.4	44.0	29.8
MNK23	-12.68	34.16	514	2004	29.38	22.12	7.26	4-Jan-18	19.89	-5.03	29.4	0.9	6.3	311.5	2.3	0.2	0.0	nm	nm	0.0
MNK24	-12.69	34.20	488	2003	41.75	36.63	5.13	8-Jan-18	17.64	13.86	29.3	2.8	6.6	716.7	4.6	0.2	1.0	10.8	5.5	0.0
MNK25	-12.70	34.20	477	2002	24.89	21.71	3.19	12-Jan-18	14.02	4.50	29.8	1.1	5.5	100.8	1.4	0.0	0.0	212.7	184.7	80.8
MNK28	-12.80	34.21	503	2013	45.72	31.74	13.99	19-Feb-18	14.05	3.70	30.9	3.9	6.6	605.7	20.1	0.2	nm	8.7	13.3	38.7
MNK35	-13.40	34.27	506	2013	29.85	23.05	6.81	16-Jan-18	10.61	5.63	29.6	3.6	5.9	274.1	3.0	0.1	3.4	98.1	86.5	nm
MNK39	-12.96	34.20	513	2008	20.70	16.08	4.62	17-Feb-18	16.43	-4.97	34.5	1.6	5.9	169.5	8.5	0.0	0.0	119.2	84.1	60.4

Table S4. Rainfall data from the rainfall collectors installed in Ethiopia (1 of 3 sites), Uganda (eight sites) and Malawi (five sites).

Addis Ababa rainfall collector		
	Monthly rainfall	Monthly average
Date	mm	Cl (mg/L)
Jan-16	59.8	1.87
Feb-16	12.1	1.31
Mar-16	47.9	2.83
Apr-16	136.8	0.78
May-16	132.7	1.13
Jun-16	187.3	1.12
Jul-16	182.8	0.98
Aug-16	299.9	0.53
Sep-16	141.8	1.55
Oct-16	15.5	1.79
Nov-16	3.6	No sample
Dec-16	1.9	No sample
Jan-17	0.0	No sample
Feb-17	20.7	3.67
Mar-17	36.6	1.80
Apr-17	33.7	1.46
May-17	0.0	0.80
Jun-17	64.5	1.02
Jul-17	290.4	1.21
Aug-17	329.8	0.54
Sep-17	386.0	0.71

Uganda rainfall collectors

	ULU02				ULU12				UBUHQ				UBU16				UBU18				UOY03				UOY13				MAK			
Month	Rainfall amount (mm)	Chloride (mg/L)	d18O	d2H	Rainfall amount (mm)	Chloride (mg/L)	d18O	d2H	Rainfall amount (mm)	Chloride (mg/L)	d18O	d2H	Rainfall amount (mm)	Chloride (mg/L)	d18O	d2H	Rainfall amount (mm)	Chloride (mg/L)	d18O	d2H	Rainfall amount (mm)	Chloride (mg/L)	d18O	d2H	Rainfall amount (mm)	Chloride (mg/L)	d18O	d2H	Rainfall amount (mm)	Chloride (mg/L)	d18O	d2H
May-17	119.5	0.51	-4.43	-23.1	48.2	0.21	-3.72	-16.9																								
Jun-17	36.8	6.8	-0.48	8.6	90.4	0.31	-1.21	4.5	58.7	0.77	0.30	13.2	76.5	0.46	-0.43	9.4	57.0	0.85	-0.20	8.6	89.7	0.60	0.03	15.1	111.5	0.49	-0.46	10.6		NO SAMPLE COLLECTED		
Jul-17	59.7	0.4	-0.53	13.1	120.1	0.28	-0.43	14.5	146.2	0.26	-0.23	14.9	148.8	0.33	-0.08	17.7	43.8	1.23	-0.54	12.5	141.1	0.24	-0.75	12.7	195.3	0.22	-0.74	12.5		NO SAMPLE COLLECTED		
Aug-17	70.0	0.4	-1.87	0.3	88.5	0.40	-2.37	-3.4	148.1	0.31	-0.84	8.1	132.0	0.24	-0.71	9.9	73.7	2.42	-0.07	6.8	245.7	0.28	-1.32	6.4	219.1	0.27	-1.42	2.5	10.3	0.39	-4.63	-22.1
Sep-17	99.9	0.2	-4.06	-19.8	106.0	0.26	-5.16	-27.1	141.3	0.31	-2.69	-7.9	118.6	0.27	-2.42	-6.0	73.7	-			165.5	0.18	-2.05	-2.2	192.3	0.39	-1.59	-0.1	97.8	0.63	-1.88	-1.1
Oct-17	89.6	5.3	-1.89	-0.9	118.8	0.53	-0.78	7.4	117.8	0.39	-0.19	9.9	81.4	0.48	-2.65	-4.6	56.5	2.99	1.07	16.3	100.7	0.50	-2.01	-2.2	195.6	0.36	-1.15	3.8	68.6	0.57	0.72	16.9
Nov-17	59.6	4.0	-2.35	-4.9	122.9	0.51	-5.90	-31.8	72.9	0.33	-4.46	-24.6	68.4	0.78	-2.79	-17.4	48.3	1.99	-2.91	-20.6	125.6	0.78	-4.84	-26.9	105.4	0.06	-3.46	-18.1	79.2	1.48	-3.49	-25.5
Dec-17	45.6	1.5	-3.48	-15.0	47.5	0.98	-1.44	2.7	9.3	2.68	0.63	18.6	11.3	2.42	1.52	10.7		NO SAMPLE COLLECTED				NO SAMPLE COLLECTED				NO SAMPLE COLLECTED			51.2	1.01	3.42	26.5
Jan-18	25.9	1.5	-3.57	-15.3		NO SAMPLE COLLECTED			10.5	2.72	0.65	19.3	1.9	20.19	15.14	70.9		NO SAMPLE COLLECTED				NO SAMPLE COLLECTED				NO SAMPLE COLLECTED			39.3	1.77	0.58	18.6
Feb-18	48.5	1.2	-1.20	1.6	47.1	1.77	-0.16	11.7	10.1	3.45	-2.07	-3.0	15.1	2.95	2.66	19.8		NO SAMPLE COLLECTED				NO SAMPLE COLLECTED				NO SAMPLE COLLECTED			40.2	1.08	1.01	10.5
Mar-18	88.1	0.7	-0.94	9.4	77.5	0.67	-0.71	10.1	79.8	0.57	-0.59	14.7	72.9	0.61	0.01	14.7	89.1	3.70	0.02	7.5	58.7	0.97	-0.97	4.5	94.7	1.25	0.34	16.5	166.9	0.56	-0.45	8.3
Apr-18	175.8	0.2	-7.69	-47.6	79.5	0.3	-9.21	-62.6	178.8	0.4	-6.51	-37.8	248.9	0.2	-7.16	-43.2	123.7	1.1	-6.04	-42.6	280.7	0.4	-2.39	-3.7	181.4	0.2	-4.85	-27.3	195.4	0.1	-8.10	-55.9
May-18	66.0	0.2	-4.86	-25.6	115.0	0.2	-5.45	-29.8	118.5	0.3	-3.81	-17.1	163.6	0.2	-4.20	-20.2	120.3	1.6	-2.64	-10.2	70.5	0.5	-2.72	-8.6	141.6	0.2	-4.23	-21.4	42.3	0.4	-2.79	-11.5
Jun-18	53.8	0.5	-0.89	8.3	57.8	0.2	-1.41	5.0	86.7	0.3	-0.75	8.2	59.5	0.4	-0.67	9.8	129.1	4.0	0.19	9.5	105.8	0.2	-0.94	7.0	106.1	0.3	-0.05	14.8	57.5	0.5	-0.11	14.8
Jul-18	37.5	0.9	-0.40	14.2	31.4	0.5	-0.58	12.9	43.5	0.5	0.68	19.6	62.3	0.9	0.72	18.6	13.7	3.3	4.56	35.1		NO SAMPLE COLLECTED			44.3	0.8	0.39	17.2	57.0	0.6	-0.21	14.4

Malawi rainfall collectors				
Date	District	Community	Rainfall amount (mm)	Chloride (mg/L)
May-17	Lilongwe	Nyanga	8	21
Jun-17	Lilongwe	Nyanga	2	0.50
Jul-17	Lilongwe	Nyanga	2	0.66
Oct-17	Lilongwe	Nyanga	9	1.4
Feb-18	Lilongwe	Nyanga	199	0.2
Mar-18	Lilongwe	Nyanga	128	0.2
May-18	Lilongwe	Nyanga	8	0.4
Jun-17	Lilongwe	Makanga	2	0.08
Jul-17	Lilongwe	Makanga	2	3.0
Oct-17	Lilongwe	Makanga	9	5.1
Nov-17	Lilongwe	Makanga	65	1.2
Dec-17	Lilongwe	Makanga	175	4.4
Feb-18	Lilongwe	Makanga	199	0.2
May-18	Lilongwe	Makanga	8	0.8
Oct-17	Lilongwe	Mtowavibvi	9	0.40
Nov-17	Lilongwe	Mtowavibvi	65	0.81
Dec-17	Lilongwe	Mtowavibvi	175	5.6
Feb-18	Lilongwe	Mtowavibvi	199	0.2
May-18	Lilongwe	Mtowavibvi	8	0.7
Jun-17	Balaka	Chipapa	5	1.8
Jul-17	Balaka	Chipapa	5	2.0
Mar-18	Balaka	Chipapa	148	0.4
Jun-18	Balaka	Chipapa	5	3.9
May-17	Lilongwe	Chimwayi	8	1.4
Jun-17	Lilongwe	Chimwayi	2	1.5
Jul-17	Lilongwe	Chimwayi	2	0.71
Oct-17	Lilongwe	Chimwayi	9	0.47
Dec-17	Lilongwe	Chimwayi	175	4.5

REFERENCES

Busenberg, E., Plummer, L.N., 2000. Dating young groundwater with sulfur hexafluoride: Natural and anthropogenic sources of sulfur hexafluoride. Water Resources Research, 36(10): 3011. DOI:10.1029/2000WR900151

Cook, P.G., Solomon, D.K., Plummer, L.N., Busenberg, E., Schiff, S.L., 1995. Chlorofluorocarbons as Tracers of Groundwater Transport Processes in a Shallow, Silty Sand Aquifer. Water Resources Research, 31(3): 425-434. DOI:10.1029/94wr02528

Heaton, T.H.E., Vogel, J.C., 1981. "Excess air" in groundwater. Journal of Hydrology, 50(0): 201-216. DOI:10.1016/0022-1694(81)90070-6

Kebede, S., 2012. Groundwater in Ethiopia: Features, Numbers and Opportunities. Springer Berlin Heidelberg.

Kebede, S. et al., 2019. Physical factors contributing to rural water supply functionality performance in Ethiopia, Nottingham, UK.

Kebede, S., Travi, Y., Alemayehu, T., Ayenew, T., 2005. Groundwater recharge, circulation and geochemical evolution in the source region of the Blue Nile River, Ethiopia. Applied Geochemistry, 20(9): 1658-1676. DOI:10.1016/j.apgeochem.2005.04.016

Maiss, M., Brenninkmeijer, C.A.M., 1998. Atmospheric SF6: Trends, Sources, and Prospects. Environmental Science & Technology, 32(20): 3077-3086. DOI:10.1021/es9802807

Mapoma, H.W.T., Xie, X., 2014. Basement and alluvial aquifers of Malawi: An overview of groundwater quality and policies. African Journal of Environmental Science and Technology, 8(3): 190-202.

Maurice, L. et al., 2019. Characteristics of high-intensity groundwater abstractions from weathered crystalline bedrock aquifers in East Africa. Hydrogeology Journal, 27(2): 459-474. DOI:10.1007/s10040-018-1836-9

Mwathunga, E. et al., 2019. Physical factors contributing to rural water supply functionality performance in Malawi, Nottingham, UK.

NOAA, 2019. Combined Chloroflurocarbon-12, Chloroflurocarbon-11 and Sulphur hexafluoride data from the NOAA/ESRL Global Monitoring Division.

Ó Dochartaigh, B.É., 2019. User Guide: Africa Groundwater Atlas Country HydrogeologyMaps, Version 1.0. BritishGeological Survey Open Report, OR/19/035, British Geological Survey.

Oster, H., Sonntag, C., Münnich, K.O., 1996. Groundwater Age Dating with Chlorofluorocarbons. Water Resources Research, 32(10): 2989-3001. DOI:10.1029/96WR01775

Owor, M. et al., 2019. Physical factors contributing to rural water supply functionality performance in Uganda, Nottingham, UK.

Poulsen, D.L., Cook, P.G., Dogramaci, S., 2020. Excess Air Correction of SF6 and Other Dissolved Gases in Groundwater Impacted by Compressed Air From Drilling or Well Development. Water Resources Research, 56(8): e2020WR028054. DOI:10.1029/2020wr028054

Schlueter, T., 2006. Geological Atlas of Africa: With Notes on Stratigraphy, Tectonics, Economic Geology, Geohazards and Geosites of Each Country. DOI:10.1007/3-540-29145-8

Sebol, L.A., Robertson, W.D., Busenberg, E., Plummer, L.N., Ryan, M.C., Schiff, S.L., 2007. Evidence of CFC degradation in groundwater under pyrite-oxidizing conditions. Journal of Hydrology, 347(1): 1-12. DOI:10.1016/j.jhydrol.2007.08.009

Smith-Carington, A.K., Chilton, J.P., 1983. Groundwater Resources of Malawi, Department of Lands, Valuation and Water/Institute of Geological Sciences, Lilongwe, Malawi.

Taylor, R., Howard, K., 2000. A tectono-geomorphic model of the hydrogeology of deeply weathered crystalline rock: Evidence from Uganda. Hydrogeology Journal, 8(3): 279-294. DOI:10.1007/s100400000069

Taylor, R.G., Barrett, M., Tindimugaya, C., 2003. Urban areas of sub-Saharan Africa: weathered crystalline aquifer systems. In: Lerner, D. (Ed.), Urban Groundwater Pollution: IAH International Contributions to Hydrogeology 24. Taylor & Francis, pp. 26.

Taylor, R.G., Howard, K.W.F., 1998. Post-Palaeozoic evolution of weathered landsurfaces in Uganda by tectonically controlled deep weathering and stripping. Geomorphology, 25(3): 173-192. DOI:10.1016/S0169-555X(98)00040-3

Tindimugaya, C., 2008. Groundwater flow and storage in weathered crystalline rock aquifer systems of Uganda: evidence from environmental tracers and aquifer responses to hydraulic stress. University of London.

United Nations Department of Economic and Social Affairs Population Division, 2018. World Urbanization Prospects: The 2018 Revision. Working Paper No. ESA/P/WP.252, New York: Unite Nations.

United Nations Department of Economic and Social Affairs Population Division, 2019. World Population Prospects 2019. Data Booklet, New York: United Nations.

von Rohden, C., Kreuzer, A., Chen, Z., Kipfer, R., Aeschbach-Hertig, W., 2010. Characterizing the recharge regime of the strongly exploited aquifers of the North China Plain by environmental tracers. Water Resources Research, 46(5). DOI:10.1029/2008wr007660

Westerhof, A.B. et al., 2014. Geology and geodynamic development of Uganda with explanation of the 1:1,000,000 scale geological map.